Biosensors and Bioelectronics 54 (2014) 661–666

Contents lists available at ScienceDirect

Biosensors and Bioelectronics

journal homepage: www.elsevier.com/locate/bios

Plastic optical fiber-based biosensor platform for rapid cell detection

Gisele Wandermur [a], Domingos Rodrigues [a], Regina Allil [b], Vanessa Queiroz [a], Raquel Peixoto [c], Marcelo Werneck [a,*], Marco Miguel [d]

[a] Photonic and Instrumentation Laboratory, Electrical Engeineering Program, Universidade Federal do Rio de Janeiro, Cidade Universitária, Rio de Janeiro, Brazil
[b] Division of Chemical, Biological and Nuclear Defence, Biological Defence Laboratory, Brazilian Army Technological Center, Rio de Janeiro, RJ, Brazil
[c] Laboratory of Molecular Microbial Ecology, Department of General Microbiology, Universidade Federal do Rio de Janeiro, Cidade Universitária, Rio de Janeiro, Brazil
[d] Food Microbiology Laboratory, Department of Medical Microbiology, Universidade Federal do Rio de Janeiro, Cidade Universitária, Rio de Janeiro, Brazil

ARTICLE INFO

Article history:
Received 14 August 2013
Received in revised form
7 November 2013
Accepted 8 November 2013
Available online 18 November 2013

Keywords:
Biosensor
Plastic optical fiber
Cell detection
Immunosensor

ABSTRACT

This work presents a novel, fast response time, plastic optic fiber (POF) biosensor to detect *Escherichia coli*. It discloses the technique for the development, calibration and measurement of this robust and simple-to-construct POF biosensor. The probes in U-shaped format were manufactured with a specially developed device. The calibration process led to the evaluation of the sensitivity, accuracy and repeatability by using solutions of sucrose for obtaining refractive indices (RI) in the range 1.33–1.39 IR equivalent of water and bacteria, respectively. The POF probes were functionalized with antibody anti-*E. coli* serotype O55 and tested firstly with saline and then with bacterial concentrations of 10^4, 10^6, and 10^8 colony forming units/ml (CFU/ml). The optoelectronic setup consists of an 880 nm LED connected to the U-shaped probe driven by a sine waveform generated by the Simulink (from Matlab®). On the other side of the probe a photodetector generates a photocurrent which is amplified by a transconductance amplifier. The output voltage signal is read by the analog-to-digital (A/D) input of the microcontroller. In all tested concentrations, the results presented a tendency of a decrease in the output signal with time, due to the attachment of the bacteria to the POF probe and consequent increase in the RI close to the sensitive area of the fiber surface. It has been shown that the system is capable of providing positive response to the bacterial concentration in less than 10 min, demonstrating good possibilities to be commercially developed as a portable field sensor.

1. Introduction

The combat against diseases is becoming an increasingly important issue in developing countries that must rely on readily available diagnostic assays. These assays need to be of easy operation and rapid response because in many environments it is important to have immediate detection of contaminants, particularly for water quality, clinical diagnosis or food safety.

On the other hand, conventional methods for pathogen detection depend on classical techniques that are time-consuming needing specialized personnel and laboratories.

However, in the last two decades we are witnessing a significant growth in biosensor technologies substituting conventional detection methods. As is widely known, biosensors rely on a biological recognition element that interacts with the target and produces a calibrated signal that is used as a parameter transducer. The output signal and hence the technology can be divided into several categories such as physicochemical, amperometric, piezoelectric, electrochemical or optical. The optical technology has recently emerged in the market, migrated from the telecom area, as a powerful, cheap and reliable tool, allowing the development of new techniques for biological detection. Optical biosensors offer several advantages when compared with their conventional electric counterparts such as electric passiveness, long distance sensing, possibility of multiplexing several sensing channels, electromagnetic immunity, etc.

For this reason, the development of new types of optical biosensors and their further use is growing fast, as shown in a review work conducted by Lazcka et al. (2007).

In a survey for more recent applications of optical biosensors it is possible to split biological detection into several different techniques: some studies detect the presence of the cells around the fiber by refraction index (RI) variation such as in Ferreira et al. (2001) and Beres et al. (2011). Some studies, such as Bharadwaj et al. (2011), use the absorbance of light as a measurement

* Corresponding author. Tel.: +55 21 25628200.
E-mail addresses: werneck@lif.coppe.ufrj.br, werneck@pq.cnpq.br (M. Werneck).

0956-5663/$ - see front matter © 2013 Elsevier B.V. All rights reserved.
http://dx.doi.org/10.1016/j.bios.2013.11.030

principle. In reality, absorbance and RI are both responsible for the light decay by absorbance and by decreasing the number of propagating modes inside the fiber core due to the higher RI of the bacteria at the fiber surface, respectively. Futhermore, Fischer et al. (2012) and Emiliyanov et al. (2013), detect the fluorescence emitted by the cells and Chai et al. (2011) present a study for detection of the enzymatic reaction caused by the presence of the bacteria.

Biological detection through RI measurements can be performed in several ways by the use of optical fiber sensors. Surface plasmon resonance (SPR) is one of these methods and is used widely as a detection principle in different fields. SPR is very attractive because it can attain resolutions as high as 10^{-7} RIU (refraction index units) (Cennamo et al., 2011). Other well-known technology is based on the light interference phenomenon and can be implemented either in optical fibers or in planar wave-guides producing accuracies as high as those produced by SPR (Fan et al., 2008).

Optical fiber grating, also known as fiber Bragg grating (FBG) is another very accurate technique for measuring RI (Baldini et al., 2012). In order to adapt FBGs to be sensitive to the RI of the surrounding medium it is necessary to expose the interface between the core and the cladding at the location where the grating was inscribed. This exposition is performed by etching or polishing the region and then it is necessary to activate the interface with the proper sensitive layer.

Evanescent wave (EW)-based biosensor is another common technique for RI measurement. It is based on the exposition of the core/cladding interface of an optical wave guide in order to promote an interaction between the EW and the surrounding medium. As will be seen in the next section, the EW occurs in the core/cladding interface, around the core. To reach the EW it is also necessary to etch or polish the fiber as seen in Sai et al. (2010). Another way to reach the EW is by tapering the fiber by heating and drawing and this can be accomplished either in silica fibers or in plastic fibers (Beres et al., 2011; Rahman et al., 2011).

As it has been shown above, the RI measurement techniques demand some previous preparation of the fiber, i.e. polishing, etching, pulling, FBG scribing, thin film deposition, etc. However, for developing a sensor probe with a larger possibility of ending up in a commercial and large scale production, it is necessary to think of simple and easy-to-fabricate sensor probes.

Now, on comparing the techniques mentioned above, either they are difficult to accomplish (taper, SPR, interferometry), expensive to fabricate (FBG) or complicated and expensive to interrogate (FBG, fluorescence).

In this work an innovative biosensor platform based on RI measurement in plastic optical fiber (POF) sensor probe is presented and experimentally tested for the presence of three different concentrations of bacterium *Escherichia coli*. Three main objectives were aimed at: determination of the best sensor configuration (namely, the POF type to be used as sensor probe), a simple method of fabricating the sensor probe and the performance evaluation of the field-portable biosensor system, functionalized for rapid detection of specific microorganisms.

2. Theory of the fiber optic biosensor

When light propagates through a wave guide, it is bound inside the core by the phenomenon of total internal reflection (TIR). Thus, there is a critical angle above which, all light rays will suffer TIR at the core/cladding interface. This angle is given by

$$\theta_c = \sin^{-1}\left(\frac{n_{cl}}{n_{co}}\right) \tag{1}$$

where n_{cl} is the RI of the fiber cladding and n_{co} that of the core. For incident angles close to θ_c there will be a small portion of the optical power extending into the cladding. This electromagnetic wave, known as the evanescent wave (EW), drops exponentially with distance from the core until its power is negligibly small. The distance from the core to the point in which the power, for all practical effects, is null, is given by (Anderson and Chris Taitt,2011)

$$d_p = \frac{\lambda}{2\pi\sqrt{n_{co}^2 \sin^2\theta - n_{cl}^2}} \tag{2}$$

where θ is the incident angle of the light ray and λ is the wavelength.

The operating principle of a taper is based on the EW enclosed inside the cladding and, by decreasing the fiber diameter by the tapering process, the EW becomes exposed. Notice that the EW will extend outside the cladding if d_p is larger than the resulting cladding thickness and in this case n_{cl} in Eq. (1) will be an average between the RI of the remaining cladding and the RI of the surrounding medium. Therefore if the fiber is immersed into the analyte, its RI will dominate the output power of light that is guided by the fiber since the critical angle controls the number of propagating mode that remains in the fiber.

When the fiber is claddless, that is, it is made of a plain PMMA cylinder, the cladding is in reality the surrounding medium, or the analyte. Therefore, the output power of this fiber is an inverse function of the analyte's RI, in the sense that, the smaller the RI, the more modes the fiber supports. As the analyte's RI increases, the fiber supports less and less modes until the RI reache that of the core. At that point the critical angle is 90°, which, in practical terms means that the fiber does not guide any light; the light rays will not respect the bends, they will propagate toward the outside of the fiber.

There is one more way of controlling the number of modes propagating inside the fiber by the surrounding medium's RI. In a straight conventional fiber with core and cladding, there is always one mode propagating in the critical angle θ_c which is the highest order mode. At a bend the propagation conditions alter and light rays which would propagate in a straight fiber are lost in the cladding because in the bend the higher modes hit the core/cladding interface with an angle smaller than θ_c and then part of the power is lost into the cladding. However, the cladding also supports a few propagating modes refilled by those lost modes from the core. At the cladding interface with the analyte there will be another critical angle so that all cladding modes hitting this interface at higher angles will be guided. However, in the curve some modes will reach the interface at angles smaller than the critical angle and will be lost into the analyte. These cladding empty modes will be immediately refilled by the core modes and some power will be lost at the end of the fiber. In this way, again, the analyte's RI will dominate the output power of light that is guided by the fiber.

If this theory holds, then a pristine, conventional POF in a U-shape form can be used as a RI sensor without the need to expose the EW. This will be confirmed later in this communication.

Due to the fact that the last technique mentioned above (U-shape plain POF) is much easier to be accomplished than the former ones, it is important to compare each one's performance as an RI sensor in order to choose the best technique for a biosensor probe, considering the fabrication processes, accuracy and resolution.

In this communication we first compared four kinds of U-shaped POF-based RI sensors in terms of sensitivity, accuracy and resolution. Then, after the activation of the best POF probe type with antibody, we tested several probes in different bacterial suspensions in order to evaluate the response time and sensitivity.

3. Materials and methods

This section presents the sensor fabrication techniques, the calibration procedures, the optoelectronic setup, the protocol for sensor activation with antibody and the technique used to test the POF probes in bacterial suspension.

The RI-based biological sensor works as following: when the POF probe with the bonded antibody at its surface is immersed into the medium with bacteria, the system, in the first place, reads the index of refraction of the medium and saline. After a few minutes, the random movement of the bacteria makes them collide with the functionalized probe and become attached to its surface. At this point the system starts reading an increasing RI due to the presence of the bacteria at the probe surface. Now, depending on the antibody efficiency and its distribution around the sensor surface, this averaged RI tends to keep rising until it would eventually reach 1.39, which is the RI of the bacteria (Beres et al., 2011). At this point the bacteria would be completely covering the sensitive part of the probe.

3.1. Sensor production

All POF probes were produced using a simple, specially designed, manually operated machine containing a U-shape matrix as shown in Fig. 1(A). During fabrication it is important not to touch the fiber, particularly the claddless ones as any grease, dust, debris or scratch could irreversibly damage the probes. The first step of the fabrication is to place the pristine fiber into the machine slot (Fig. 1B) and soften the fiber by using a hot air blower gun for about 5 s. Then the machine handle is pushed in so that the fiber is forced into the U-shape mold (Fig. 1C). After letting the fiber solidify (Fig. 1D) its extremities are cut in another mold so as to have all probes in the same size (see the cutting guillotine in Fig. 1(A) center left). Four POF probes were produced of each fiber type using this technique in order to have a good statistical average of the probe performance (Fig. 1E).

The production of the taper used the same machine, with the difference that in step C the fiber extremities are fixed while the machine's handle is pushed in. In this way the fiber stretches in a shape shown in the scanning electronic microscopy (SEM) picture Fig. 1(F).

POF probes were fabricated from four different kinds of POF as described below. Fig. 2 shows the schematic drawing of each one.

POF probe 1: Multi-mode (MM), step index (SI) POF type Mitsubishi Rayon Eska CK-40. This is a conventional telecom POF with a pure poly-methyl-methacrylate (PMMA) core and a doped low-index-of-refraction fluoropolymer as cladding. The fibers present 980 μm of core diameter and a 10 μm thickness cladding (Fig. 2A). This probe will be identified from now on as plain probe.
POF probe 2: Pure PMMA claddless fiber with 0.45 mm diameter obtained from Sojitz Europe plc, Düsseldorf (Fig. 2C).
POF probe 3: Pure PMMA claddless fiber with 1 mm diameter obtained from the University of Washington at Seattle, Department of Mechanical Engineering (Fig. 2-A).
POF probe 4: Same material as POF probe 1 with a taper (Fig. 2B).

3.2. Sensor calibration

In order to calibrate the sensors and evaluate their sensitivity, accuracy and repeatability we prepared several solutions of sucrose in ultrapure water (15%, 25%, 30%, 45% and 52%) and measured the RI of each solution with an Abbe refractometer for producing five calibrated solutions. Ten measurements of each solution were performed and the average RI was plotted against the concentration.

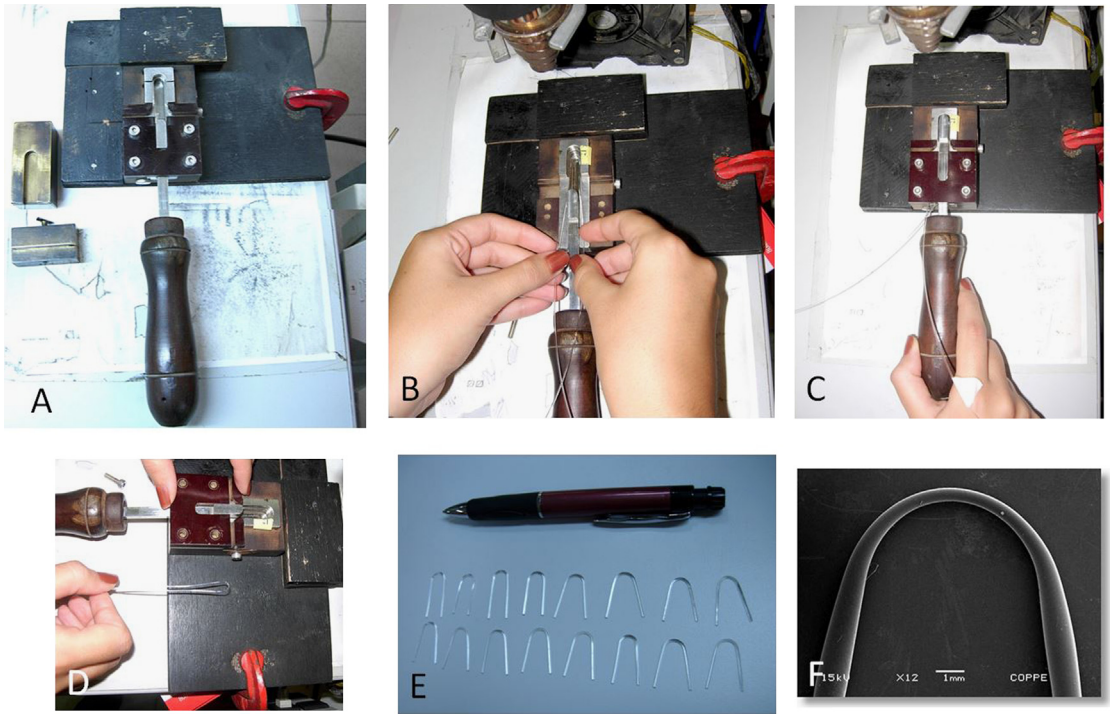

Fig. 1. Sequence of POF probes fabrication: (A) manually operated machine containing a U-shape matrix; (B) first step of the fabrication placing the pristine fiber into the machine slot and turn on the hot air blower gun; (C) the machine hand is pushed in so that the fiber is forced into the U-shape mold; (D) after fiber solidification the extremities are cut; (E) several POF probes were fabricated; and (F) SEM of the taper. Tapers were produced by holding the fiber extremities before pushing the machine handle.

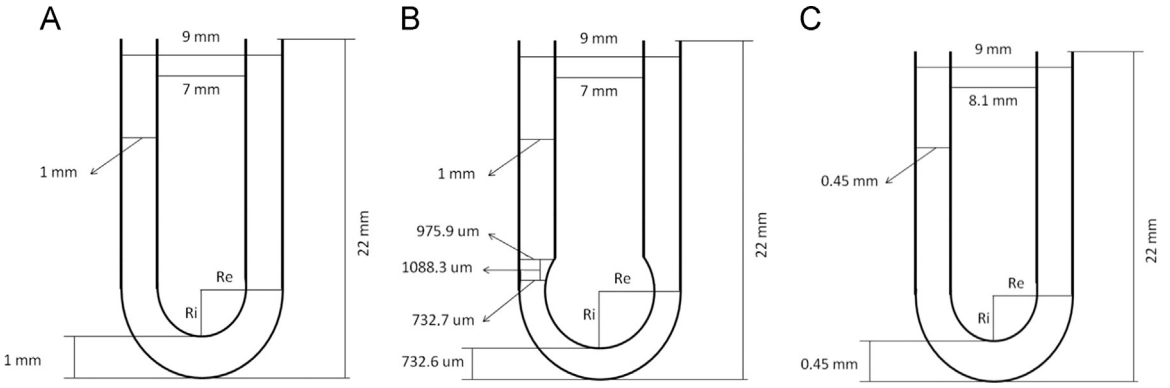

Fig. 2. Schematic drawings of the POF probes. (A) POF probe 1: MM-SI conventional telecom PMMA-POF and POF probe 3: pure PMMA claddless fiber with 1 mm diameter; (B) POF probe 4: same as POF probe 1 with a taper; and (C) POF probe 2: pure PMMA claddless fiber with 0.45 mm diameter.

During the calibration procedures, each sensor was immersed sequentially into the calibrated solutions and this was repeated until 10 sets of measurements were recorded. Then, the uncertainty parameters were calculated.

3.3. Antibody immobilization protocol

3.3.1. Sensor surface preparation

The protocol used for binding antibodies was adapted according to the methodology proposed by Fixe et al. (2004). Fiber segments were cleaned with isopropanol (99%) for 5 min, and then thoroughly washed with sterile distilled water.

3.3.2. Chemical treatment

The surface of the fibers to be aminated were incubated in a 10% hexamethylenediamine solution prepared with 100 μM borate buffer pH 11.5 for 2 h at 30 °C. After washing twice with distilled water, the fragments were dried for 2 h at 37 °C. In order to activate the amination, the fibers were added in a 2.5% glutaraldehyde solution, prepared in phosphate buffer pH 8.0, 0.1 M for 2 h at 30 °C. After this treatment the fibers were washed vigorously three times with phosphate buffer pH 8.0, 0.1 M, followed by drying for 2 h at 37 °C.

3.3.3. Antibody immobilization

Fibers were incubated with staphylococcal protein A (Sigma-Aldrich, St. Louis, USA) in sodium carbonate buffer (Na_2CO_3) 0.05 mg/ml, pH 9.5, for 1 h at 30 °C. To avoid nonspecific binding during processing, the fiber binding sites were blocked by treatment with bovine serum albumin at 0.1% in 0.85% saline solution, pH 7.0. Blocking was performed for 1 h at 30 °C under stirring. Subsequently the fibers were washed three times in 0.85% saline, pH 7.0. Finally, the treated fibers were left in contact with 600 μl suspension of antibodies anti-*E. coli* O55 (0.1 mg/ml) obtained commercially (Probac, São Paulo, Brazil) for 4 h at 30 °C, and washed three times in 0.85% saline solution.

3.3.4. Preparation of bacterial suspensions

The bacterium *E. coli* O55, used in the preparation of the suspensions was cultured in Tryptic soy agar – TSA (Biomerieux, Rio de Janeiro, Brazil) and incubated for 24 h at 37 °C. Subsequently, the growth was transferred to saline solution for each concentration. Concentrations of 10^4, 10^6 and 10^8 CFU/ml were tested individually following the McFarland turbidity standard and subsequently confirmed by plating in TSA and incubated for 24 h at 37 °C. As negative control, i.e., bacterial strains that do not react with the attached antibodies, we used suspensions of *Enterococcus faecalis* and *Klebsiella pneumoniae*.

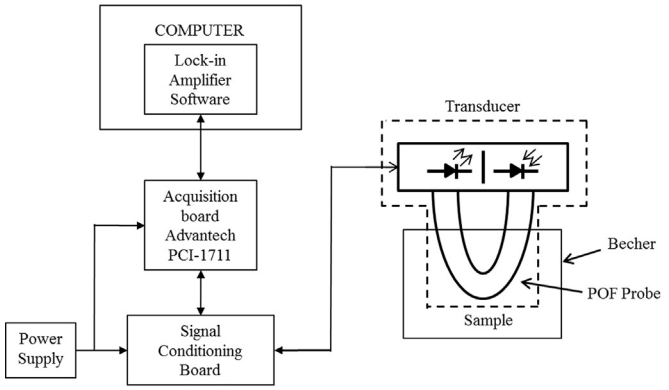

Fig. 3. Schematic diagram of the optoelectronic setup.

Readings were taken initially with a negative control immersing each sensor in 6 ml of saline, to stabilize the data of the readings at 1 min intervals for 5 min. Then each individual sensor was immersed in a bacterial suspension of specified concentration. The readings were performed in triplicate with individual sensors for each concentration of suspension. The data readings were obtained at 1 min intervals during 40 min for each sequential sensor.

In all tests the suspension was manually homogenized. Also, a negative control with saline and without bacteria was tested before the immersion in a 5 ml-glass beaker. with bacterial suspension and the readings were used for data normalization.

3.4. Instrumentation and electronic setup

The optoelectronic setup shown in Fig. 3 consists of an 880 nm LED connected to the end of the U-shaped POF probe driven by a sine waveform generated Simulink®, a simulation platform provided by Matlab®. The light from the LED is received by the photodiode located on the opposite fiber end. Both the LED and the photodetector are embedded into a block of black polyacetal, so as to avoid light leaking into the photodetector. The photodetector produces a photocurrent which is amplified by a low noise transconductance amplifier. The output voltage is fed into the microcontroller A/D input port, while output data is sent via USB to the PC where the acquisition software is run. The Simulink® communicates with the circuit through the acquisition board Advantech PCI-1711 with 12 bits; this signal is tracked and recovered without noise by a lock-in algorithm also developed in Simulink®, thus avoiding external light interferences and allowing a larger amplification since the lock-in algorithm is noise-free.

4. Results and discussion

This section presents the results and discussion of the two blocks of experiments: uncertainty assessment of the POF probes as RI sensors and sensitivity of functionalized probes as *E. coli* sensor.

4.1. POF probe as RI sensor: accuracy, resolution and precision

In this experiment each POF probe was subjected sequentially to the calibrated samples with different sucrose concentrations, ranging from pure water up to the index of refraction of 1.39, according to the experiments of Beres et al. (2011).

We made five samples of each POF probe type and a sequence of ten tests for each sensor was performed. Fig. 4 shows the averaged results for each POF probe.

Mathematical modeling was performed based on the experimental data according to GUM (2008). By analyzing the coefficients of determination of each curve adjustment, it was possible to determine the uncertainties and sensitivities. The sensitivity (S) is the first derivative of the curve with respect to the RI, that is

$$S = \frac{\partial V_{out}}{\partial RI} \tag{3}$$

Table 1 shows the calculated parameters.

As expected from Eq. (1), the output light power of the POF probes is inversely proportional to the RI of the surrounding medium. The output power tends to zero when the RI of the surrounding medium tends to that of the core (RI = 1.49) because in this case the light would not be guided by the fiber in the bend. Also, the proposed explanation for the external RI sensitivity of the plain fiber mentioned in Section 1 seems to be valid.

It was also expected that the sensitivity of claddless fiber would be better than that of the cladded ones because of the larger exposition of the evanescent field. This in fact occurred, since the 1 mm claddless POF probe sensitivity is larger than that of the tapered probe which, in turn, is larger than that of the plain fiber probe.

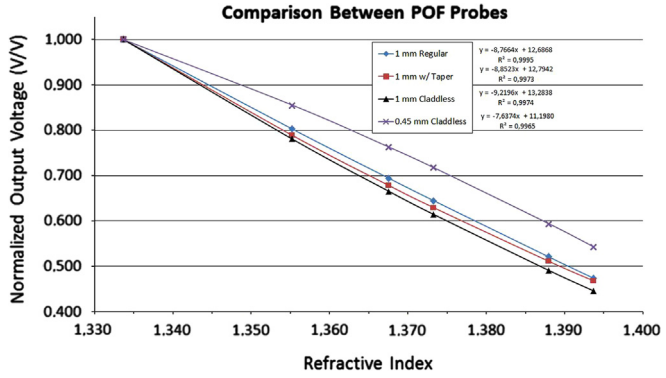

Fig. 4. Normalized output voltage of each plastic optical fiber probe when measuring calibrated solutions of sucrose. The box shows linear regression equation for each curve and the respective regression coefficient.

Table 1
Comparison of average results of uncertainties and sensitivities of the plastic optical fiber probes.

Type of POF probe	Uncertainty in RI	Sensitivity Eq. (3)
1 mm claddless	0.8×10^{-3}	9.22
1 mm with taper	0.6×10^{-3}	8.85
1 mm plain	0.5×10^{-3}	8.76
0.45 mm claddless	1.0×10^{-3}	7.64

The 0.45 mm claddless probe presented an anomalous sensitivity which can be concluded by the worst accuracy and regression coefficient (see Table 1 and Fig. 4). This can be attributed to the fact that due to the smaller diameter, this fiber guides less light that in the end, leads to a poorer signal-to-noise ratio in the detector signal. In reality this POF-probe presented the worst accuracy as seen in Table 1. Therefore this POF probe type is not appropriate to be used as a sensor.

From Table 1 it can be seen that the three remaining sensitivities do not vary more than about 5% among each other. This can be explained by noticing that for a accentuated fiber bending, the effect of Eq. (1) prevails over the effect of the EW exposition.

Comparing now the uncertainties, the claddless probes tend to be worse than the cladded ones. We experienced this situation when testing the probes by dipping them inside the glass beaker containing the calibrated solutions. A small difference in the liquid level around the fiber is enough to change the output voltage. This is because in the cladded fibers the sensitive part is on the bend, whereas the claddless fibers are sensitive all over their length as the EW is exposed all the way from beginning to the end of the fiber. So anything touching the fiber, either water, moisture, droplets or any debris is sufficient to change its responsivity.

Therefore, since the sensitivity difference is negligible the obvious choice for the better probe is the plain fiber POF probe which also presents better uncertainty and is the simplest to produce.

In order to calculate the resolution of the POF probes we first notice that the RI measurement range is between about 1.33 (pure water) and 1.39 (pure bacteria), that is 0.06 RIU. Now, recall that the uncertainty limits the resolution, as small variations of the analyte in a range below the uncertainty are not seen by the system. Therefore we can infer the resolution by these two parameters. The best resolution will be provided by the POF probe with smaller uncertainty that is the plain POF probe, with an uncertainty of 0.5×10^{-3}. Now, if we divide 0.06 by 0.5×10^{-3} we get 120 levels of detection. This means that with this probe it will be possible to have a scale of 120 different readings for water contamination.

Finally, it is worth mentioning that the accuracy found for the 1 mm plain sensor is about the same order of magnitude as that of the Abbe refractometer proving that the developed system works well as a RI meter.

To the best of our knowledge, the works available in the literature, although dealing with fiber optic sensors for refractive index measurements, are not focused in the accuracy or sensitivity of their systems, such as the studies of Wong et al. (2003) and Beres et al. (2011). Therefore it is very difficult to evaluate and compare our results. In reality, the purpose of the present work is not to reach a high degree of accuracy in RI measurement; it is, rather, to determine the resolution of our system when detecting the presence of different concentrations of bacteria in water.

4.2. Biological sensing

The plain POF probe was functionalized with antibody anti-*E. coli* O55 as described above and tested with several bacteria suspensions. The results shown in Fig. 5 are the average of three different experiments with different fibers.

In all concentrations there was a tendency of a decrease in the output signal along the time. This is explained by the attaching of the bacteria to the POF probe and thus increasing the RI close to the fiber surface.

The sensor did not respond to the negative control, composed of suspensions of 10^8 cell per milliliter of *E. faecalis* and *K. pneumoniae*. As is well known, *K. pneumoniae* also belongs to the coliform group as much as *E. coli* and is generally used as a water quality indicator

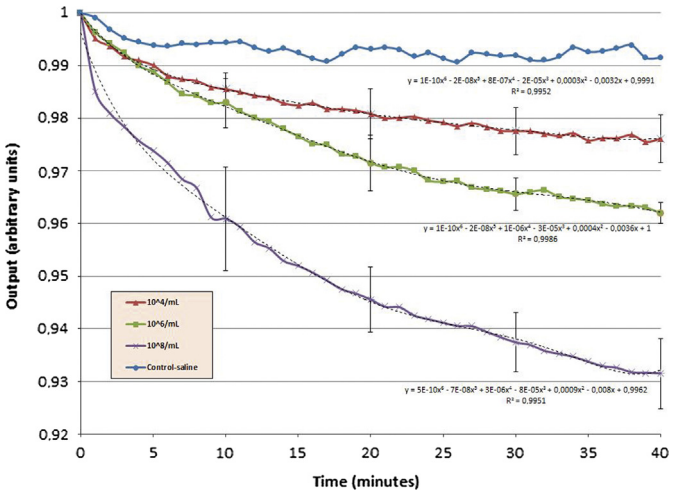

Fig. 5. Results for the tests with *Escherichia coli* O55 for 10^4, 10^6, and 10^8 CFU/ml and saline as negative control. A 6th order polynomial regression (dotted line) is also shown along with its correlation coefficient (CFU: colony forming units).

and *E. faecalis* although used as an indicator, is not taxonomically related to *E. coli*. This demonstrates the sensor specificity to *E. coli*.

Notice that the higher the bacteria concentration the more rapidly the output signal decays. In order to quantify the concentration from the system readings there seem to be two options.

The first option is to wait for a reading saturation, that is, until there are no more bacteria available close to the POF probe to be attached. This minimum value can be proportional to the bacteria concentration. This method, however, will demand a waiting of up to 1 h to have a positive response.

As for the second method, notice that the higher concentration curves decay quicker than the lower concentration. Therefore, one can calculate the first derivative of the decaying curve at origin and relate it to the concentration. Fig. 5 shows the 6th order polynomial regression and each correlation coefficient, demonstrating a very good fit ($R^2 > 0.99$ in all cases). By derivating these equations at the origin we get the decaying parameters of 3.0×10^{-3}, 3.6×10^{-3} and 8.0×10^{-3} for concentrations of 10^4, 10^6 and 10^8, respectively. These coefficients can be used as calibrating parameters for a future field prototype.

5. Conclusions

A novel and universal optical sensing platform, composed of a simple POF probe was constructed and functionalized as a biosensor for rapid and real-time specific detection of *E. coli*. The technique employed in the construction of this biosensor fulfills the requirements of easy handling, robustness and simple construction.

It has been demonstrated that the application of U-shaped sensor probes can afford several advantages, such as increased sensitivity, smaller taper length, economic use of reagents, and improved handling and fabrication leading to a greater mechanical resistance.

With respect to sensitivity it has been shown that the higher the bacterial concentration, the higher the antigen–antibody attachment speeds. Therefore the first derivative of the RI curve with respect to time can be used as a parameter to evaluate the bacterial concentration.

More tests are under way to improve the system sensitivity in order to become competitive with other existing systems for pathogen detection, such as in the range of 10^2 cells per milliliter of solution.

Acknowledgments

The authors gratefully acknowledge Dr. Peter Kröplin from Sojitz Europe plc, Düsseldorf, who provided the 0.45 mm claddless PMMA fiber and Prof. Ann Mescher from the University of Washington at Seattle, Department of Mechanical Engineering, who provided the 1 mm claddless PMMA fiber.

References

Anderson P. George , Chris Rowe Taitt, Evanescent wave fiber optic biosensors today and tomorrow, 2nd edn, In: Frances S. Ligler, Chris Rowe Taitt, (Eds.) Optical Biosensors (Chapter 2), ISBN:978-0-444-53125-4.

Baldini, F., Brenci, M., Chiavaioli, F., Giannetti, A., Trono, C., 2012. Anal. Bioanal. Chem. 402, 109–116.

Beres, C., Nazaré, F.B.V., Souza, N.C.C., Miguel, M.A.L., Werneck, M., 2011. Biosens. Bioelectron. 30, 328–332.

Bharadwaj, R., Sai, V.V.R., Thakare, K., Dhawangale, A., Kundu, T., Titus, S., Verma, P.K., Mukherji, S., 2011. Biosens. Bioelectron. 26, 3367–3370.

Cennamo, N., Massarotti, D., Conte, L., Zeni, L., 2011. Sensors 11, 11752–11760.

Chai, C., Liu, G., Yao, B., 2011. Sens. Actuators B 152, 1–7.

Emiliyanov, G., Hoiby, P.E., Pedersen, L.H., Bang, O., 2013. Sensors 13, 3242–3251.

Fan, X., White, I.M., Shopova, S.I., Zhu, H., Suter, J.D., Sun, Y., 2008. Anal. Chim. Acta 620, 8–26.

Ferreira, A.P., Werneck, M.M., Ribeiro, R.M., 2001. Biosens. Bioelectron. 16, 399–408.

Fischer, M., Wahl, M., Friedrichs, G., 2012. Biosens. Bioelectron. 33, 172–178.

Fixe, F., Dufva, P., Telleman, M., Christensen, C.B.V., 2004. Nucl. Acids Res. 32 (No. 1), 9.

Lazcka, O., Del Campo, F.J., M~unoz, F.X., 2007. Biosens. Bioelectron. 22, 1205–1217.

Rahman, H.A., Harun, S.W., Yasin, M., Phang, S.W., Damanhuri, S.S.A., Arof, H., Ahmad., H., 2011. Sens. Actuators A: Phys. 171 (2), 219–222.

Sai, V.V.R., Kundub, T., Titusc, S., Kumarc, P., Mukherjia, S., 2010. Sens. Actuators B 143, 724–730.

GUM, 2008. Evaluation of measurement data—guide to the expression of uncertainty in measurement, produced by Working Group 1 of the Joint Committee for Guides in Metrology (JCGM/WG 1), Bureau International des Poids et Mesures. Available from: ⟨http://www.bipm.org/en/publications/guides/gum.html⟩.

Wong, Y.M., Scully, P.J., Kadim, H.J., Alexiou, V., Bartlett, R.J., 2003. J. Opt. A: Pure Appl. Opt. 5, 51–58.